Proceedings of the ASME 2017 36th International Conference on Ocean, Offshore & Arctic Engineering
OMAE 2017
June 25-30, 2017, Trondheim, Norway

OMAE2017-61742

UNDERWATER POSITIONING USING NEAR SURFACE LONG BASELINE TRANSPONDER'S INDUCED BY WAVE MOTION

Stian S. Sandøy
NTNU Norwegian University
of Science and Technology
Department of Marine Technology
Trondheim 7052, Otto Nielsensvei 10
Email: stian.s.sandoy@ntnu.no

Ingrid Schjølberg
NTNU Norwegian University
of Science and Technology
Department of Marine Technology
Trondheim 7052, Otto Nielsensvei 10
Email: ingrid.schjolberg@ntnu.no

ABSTRACT

This paper presents a filter for underwater positioning in an aquaculture environment with demanding weather conditions. The positioning system is based on acoustic transponders mounted at a net pen on the sea surface. The transponders are exposed to oscillations due to wave disturbance. This will have an impact on the accuracy of the positioning system. An extended Kalman filter (EKF) solution has been proposed including a wave motion model integrated with the pseudo-range measurements from the transponders. Simulations show that the proposed filter compensates well for the disturbances.

1 Introduction

1.1 Background and Motivation

Recently, there has been an increased interest in exposed aquaculture due to environmental and spatial limitations in more sheltered areas [1]. Remoteness and harsh environments motivate the use of Underwater Vehicles (UV) in inspection, maintenance, and repair (IMR) operations. Positioning and localization are key technologies for enabling such operations. Global Navigation Satellite Systems (GNSSs) cannot be used under water. However, other technologies like long baseline (LBL), short baseline (SBL) and ultra short baseline (USBL) systems are available [2]. LBL systems use the same principle as GNSS, namely multiple transponders measuring the distance to a receiver, also known as a pseudo-range measurement. Current LBL systems are expensive and mounted on the sea-bed, which is not optimal in an aquaculture environment. In the aquaculture industry, the overall goal is to reduce on-site manual operations for increased safety and reduced risk for workers [3]. Moreover, to keep the cost of installation, operation and maintenance low. One way of doing this is increased use of remote operations and UVs. For efficient UV operations, there is a need for an underwater positioning system. The configuration of an acoustic transponder system for range measurements is a key challenge and is further assessed. The main idea behind this work is to analyze and reduce negative effects that motion in near surface transponders has on a positioning system. The motion is caused by environmental disturbances like current or waves and can create large errors in the position estimate if not contracted. It is essential that this error is as small as possible to ensure an accurate positioning of the UVs.

1.2 Literature review

There has been a considerable amount of work in navigation, which is meant as finding a position relative to some reference [4]. Especially for GNSS/Inertial Navigation System (INS) [21]. However, the environmental disturbance like ocean current and waves on transponders has not been discussed, and is highly relevant in an aquaculture setting near the ocean surface. Surveys on underwater navigation [5, 6] discuss the sensors available, their accuracy and how state estimation can be applied to fuse sensor information together using both dead reckoning

sensors like accelerometers and gyros to find orientation. A celebrated nonlinear filter for the latter is the complementary filter from [7] and later enhanced in [8] to an attitude observer. A widely used extended Kalman filter (EKF) approach is presented in [9]. Other, various translation observers using Kalman filter (KF) approaches are discussed in literature like [10]. Examples are Unscented KF, Ensemble KF and particle filter. However, in general, the nonlinear KF's are not proven globally stable in estimating position by pseudo ranges. Recently there has been a suggestion to transform the problem into a quasi-linear. The transformation was first suggested in [11]. Use for KF was first developed in [12], which made the implemented observer Global Exponential Stable (GES), but the transformation is optimal with noisy measurements. This can be resolved by using the Exogenous KF (XKF) presented in [13]. The KF using the quasi-linear model are here used as a linearization point for the next KF inheriting the stability properties and the noise reduction. A complete implementation for navigation using pseudo-range measurements is presented in [14]. Later, it has been implemented in combination with attitude filter in [15] using the attitude filter from [8]. However, this implementation dose not account for the biases in LBL systems. This is implemented using the three stage filter in [16, 17]. Study of wave motions and sea states has been a wide research field. Examples can be found in [18–20].

1.3 Main Contribution and Structure

The main contribution of this paper is the integration of a wave filter model with pseudo-range measurements. This is an important contribution since it enables mounting of transponders near the ocean surface on aquaculture structures, without having the need to calculated the position in real time with GNSS. The solution is simulated with measurements from a LBL system setup near the ocean surface, assuming that the mean transponder position is known and there are only oscillating perturbations. Each measurement correlates and can, therefore, be estimated as a single oscillating term.

This paper will first present the problem statement in Section 2. Further in 3, will necessary mathematical models for the problem at hand be designed. From this will Section 4, develop an extended Kalman filter for each case. Results and discussion are presented in sections 5 and 6, followed by conclusion in Section 7.

1.4 Notation

$(\cdot)^T$ is the transposed of a vector or matrix, and $||\cdot||$ is used as the euclidean norm. As the set of real numbers are noted as $\mathbf{R}^{n\times m}$ with the dimension $n \times m$, where no indication $\mathbf{R}$, implies $m = 1$ and $n = 1$. $0_{p\times q}$ and $I_{p\times q}$ are the zero and identity matrix respectively, with dimension $p \times q$. Position will always

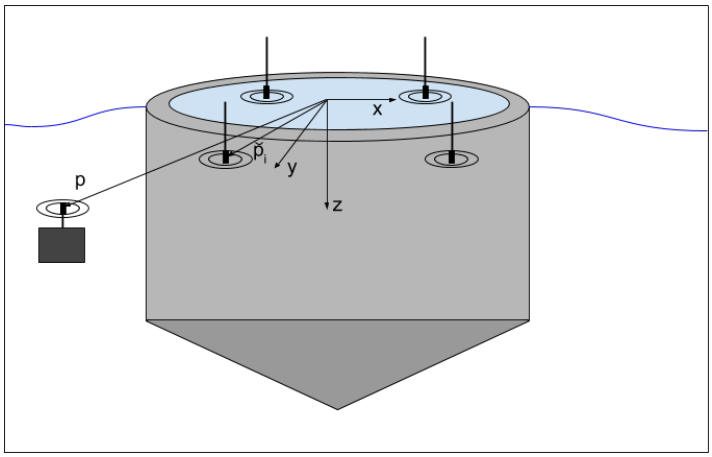

FIGURE 1: **TRANSPONDER CONFIGURATIONS**

be denoted as a vector $p = \begin{bmatrix} x & y & z \end{bmatrix}^T \in \mathbf{R}^{3\times 1}$ where x is surge, y is sway and z is heave. Wave motion vector will be designated $p_w = \begin{bmatrix} x_w & y_w & z_w \end{bmatrix}^T \in \mathbf{R}^{3\times 1}$. $N(0,\sigma^2)$ is a Normal Gaussian distribution with variance σ^2 and mean zero. $\hat{(\cdot)}$ is the notation for an estimated variable. For a matrix A and value x_i, $A = diag(x_1,\ldots,x_n) \in \mathbf{R^{n\times n}}$ means a matrix with diagonal terms x_1 to x_n and zeros everywhere else. For a function $h(x)$ and vector x, $\frac{\partial h(x)}{\partial x}$ is notation for the partial derivative.

2 Problem Statement

The problem of oscillating transponders will be studied in an aquaculture environment around a net pen as seen in Figure 1. Two cases will be discussed. In the former case denoted as A, transponders are rigidly mounted, which is the standard case for a LBL system. In the latter case denoted as B, are transponders mounted near the ocean surface. The case is illustrated in Figure 1. The main difference in these configurations is the near ocean surface disturbance's from wave motion. Here will two different measurement equations describe this deviation. The following section presents these and their assumptions. It should also be mentioned that the reference frame has an origin in the fish cage center at the mean sea surface. Positive z-axis points towards the sea floor and x-axis north. The y-axis complete the right hand, meaning eastward. This is known as the North-East-Down (NED) reference frame [20].

3 Mathematical Modeling

This section presents the mathematical models applied in the EKF. Both measurement and process model equations, are given in this section.

3.1 Measurement Model

Case A: Rigidly Mounted Transponders

Equation (1) assumes that the position for each transponder is known, as stated in Assumption 1. The measurement model is the same formulation as in [16].

$$y_i = \frac{1}{\sqrt{\beta}}(||p - \breve{p}_i|| + \varepsilon_m) = h_i(x) \tag{1}$$

Each pseudo-range measurement from transponder i is noted as $y_i \in \mathbf{R}$. The ROV and transponder position are p and $\breve{p}_i$, respectively. $\beta \in \mathbf{R}$ is a multiplicative bias which account for bias in the speed of sound in water as discussed in [16]. Measurement noise for each transponder is written as $\varepsilon_m \in \mathbf{R}$ in $N(0, \sigma_m^2)$.

Assumption 1. *The transponder position $\breve{p}_i$ is known.*

Case B: Surface Mounted Transponders

The measurement model applied for each pseudo-range from transponder "i" with position $\breve{p}_i$ is modeled in the following equation:

$$y_i = \frac{1}{\sqrt{\beta}}(||p - \breve{p}_i - \breve{p}_{wi}|| + \varepsilon_m) = h_i(x) \tag{2}$$

Equation (2) is similar to (1) with the exception of wave motion term, denoted as $\breve{p}_{wi} \in \mathbf{R}^{3\times 1}$. It assumes that the mean transponder position is known as $\breve{p}_i$ and it is subjected to time varying oscillations, denoted as $\breve{p}_{wi}$. However, each motion $\breve{p}_{wi}$ can correlate when placed in a pattern around a fish cage. So estimating all of them will be a waste of computational power. Also, the assumption of uncorrelated process noise in the KF would be violated leading to suboptimal estimates. Therefore, it is simplified to only one wave motion vector p_w, as following:

$$y_i = \frac{1}{\sqrt{\beta}}(||p + p_w - \breve{p}_i|| + \varepsilon_m) = h_i \tag{3}$$

This rough simplification can be justified not only by correlating motion and computational power. If we assume another wave motion spectra different from the transponders, can p_w estimate the oscillations that would be induced in the position estimate without it. Effectively, this can lead to an increased performance without adding too many additional computations or sensors. Finding this spectrum will not be performed here, but a simulation example will be presented in Section 5.

Assumption 2. *The mean transponder position $\breve{p}_i$ is known and the wave frequency spectrum from each transponder can be modeled as a single wave spectrum denoted p_w.*

Mark that for both Case A and B the full measurement vector is denoted as $y = h(x) = \begin{bmatrix} h_1 & \dots & h_m \end{bmatrix}^T \in \mathbf{R}^{m\times 1}$.

3.2 Process Model

Case A and B: Kinematic Model

The EKF process model requires kinematic equations of motion of the vehicle. This model will be the same for Case A and B. The velocity will be modeled as a random walk as following:

$$\dot{p} = A_p p + \varepsilon_p \tag{4}$$

Where $\varepsilon_p \in \mathbf{R}^{3\times 1}$ is $N(0, \sigma_p^2)$ and $A_p = 0_{3\times 3}$. Random walk is used because this case study only takes into account pseudo-range measurements. The velocity is not estimated in this case. It should be remarked that it is simple to also include a velocity state by including accelerometer measurements directly in the process model [14]. This would also improve the position estimates, of course depending on the quality of the accelerometer. However, since this is not the purpose of this paper, it is not taken into account. Only having position estimates also make it possible to further include this in a loosely coupled observer [21].

Case A and B: Bias Model

The sound speed bias in water, β, which are both in Case A and B will be modeled in the same manner as [16], ie. as the following:

$$\dot{\beta} = A_\beta \beta + \varepsilon_\beta \tag{5}$$

Where $A_\beta = 0$ and $\varepsilon_\beta \in \mathbf{R}$ is $N(0, \sigma_\beta^2)$. Note that this is a random walk process.

Case B: Second Order Wave Motion Model

The goal of the wave motion model presented in this section is to separate the low and wave frequency motions. This is illustrated in Figure 2. The blue dashed line is the combined low and wave frequencies, while the red solid and yellow dash-dot line are the separated low and wave frequency motions, respectively. Here is the second-order wave model used for the separation of p and p_w given in Equation (3). This model originated in [19] and can also be found in newer literature [20]. The model is given as following:

$$\begin{bmatrix} \dot{\zeta} \\ \dot{p}_w \end{bmatrix} = A_w \begin{bmatrix} \zeta \\ p_w \end{bmatrix} + E_w \varepsilon_w \in \mathbf{R}^{6\times 1} \tag{6}$$

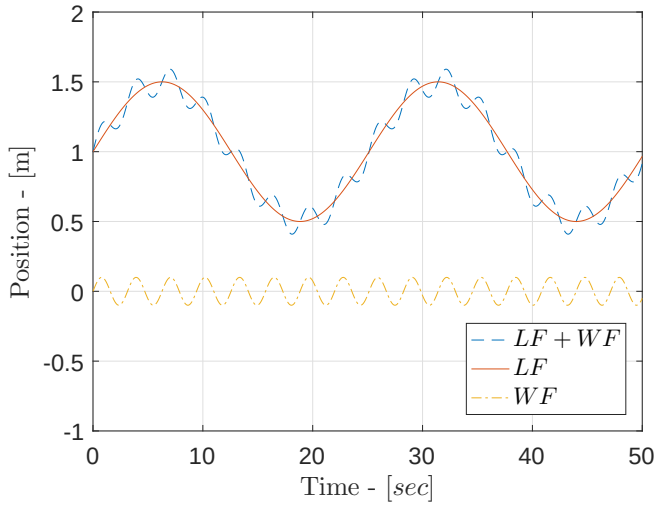

FIGURE 2: **LOW (LF) AND WAVE FREQUENCY (WF) MOTIONS** [20].

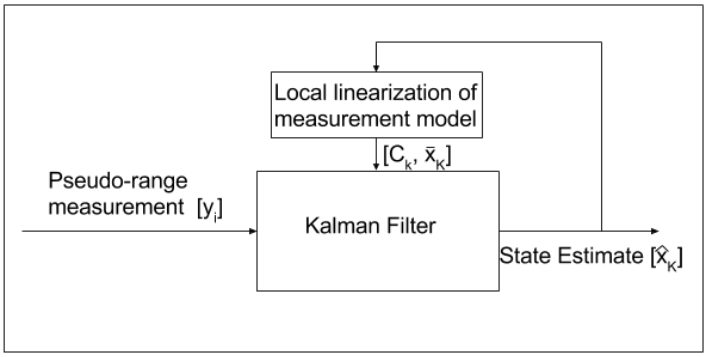

FIGURE 3: **GENERAL STRUCTURE OF EKF** [4].

where $\varepsilon_w \in \mathbf{R}^{3\times1}$ and each noise term is $N(0,1)$. Further, the matrices are defined as the following:

$$A_w = \begin{bmatrix} 0_{3\times3} & I_{3\times3} \\ -\omega_0^2 I_{3\times3} & -2\lambda\omega_0 I_{3\times3} \end{bmatrix}, E_w = \begin{bmatrix} 0_{3\times3} \\ K_w \end{bmatrix}$$

where $K_w = diag(\sigma_{w1}, \sigma_{w2}, \sigma_{w3}) \in \mathbf{R}^{3\times3}$.

4 Extended Kalman Filter's Design

The general structure of the EKF for pseudo-range measurements is described in Figure 3 [10]. The filter estimate feedback $\bar{x}_k$, generates a linearized measurement matrix called C_k. Initially in the first iteration $k = 0$, a guess $\bar{x}_0$ is used. The process and measurement equations will in this section be put together to fit the cases. Discrete process model will be defined as following:

$$\dot{x}_k = Ax_{k-1} + D\varepsilon_k \tag{7}$$

where x_k is the state vector, A is the transition matrix, D is the noise driver matrix and ε_k is the noise vector with uncorrelated white noise terms which is $N(0,\sigma^2)$. The process model of Case A will be on state space form from both Equation (4) and (5). These leads to the following state and noise vectors:

$$x = \begin{bmatrix} p \\ \beta \end{bmatrix}, \varepsilon = \begin{bmatrix} \varepsilon_p \\ \varepsilon_\beta \end{bmatrix}$$

From this it is easy to find the A and D matrix, remark that it needs to be discretized before use in the EKF. Process model of Case B is only an extension of the previous system. The state and noise vectors are defined as following:

$$x = \begin{bmatrix} \zeta \\ p_w \\ p \\ \beta \end{bmatrix}, \varepsilon = \begin{bmatrix} \varepsilon_w \\ \varepsilon_p \\ \varepsilon_\beta \end{bmatrix}$$

Also here are the corresponding A and E matrices easy to derive and is therefore not stated.

For the EKF it is also necessary to have a measurement matrix C_k. This is found by taking the Jacobian of Equation (1) for Case A and (3) for B. This is defined as following:

$$C_k = \frac{\partial h(x)}{\partial x} = \begin{bmatrix} C_{k,1} \\ \vdots \\ C_{k,m} \end{bmatrix} \in \mathbf{R}^{m\times10}$$

where m is the number of pseudo-range measurements. For Case A will the C_k matrix be:

$$C_{k,i} = \frac{\partial h_i(x)}{\partial x}\Big|_{\bar{x}} = \left[\frac{p-\check{p}_i}{\sqrt{\beta}||p-\check{p}_i||} \quad -\frac{||p-\check{p}_i||}{2\beta^{\frac{3}{2}}} \right]\Big|_{\bar{x}} \in \mathbf{R}^{1\times4}$$

And for each row in Case B it is as following:

$$C_{k,i} = \frac{\partial h_i(x)}{\partial x}\Big|_{\bar{x}} = \left[\frac{\partial h_i}{\partial \zeta} \; \frac{\partial h_i}{\partial p_w} \; \frac{\partial h_i}{\partial p} \; \frac{\partial h_i}{\partial \beta} \right]\Big|_{\bar{x}}$$

Where

$$\frac{\partial h_i}{\partial \zeta}\Big|_{\bar{x}} = 0_{1\times 3}$$
$$\frac{\partial h_i}{\partial p_w}\Big|_{\bar{x}} = \frac{\partial h_i}{\partial p}\Big|_{\bar{x}} = \frac{p+p_w-\breve{p}_i}{\sqrt{\beta}||p+p_w-\breve{p}_i||}\Big|_{\bar{x}}$$
$$\frac{\partial h_i}{\partial \beta}\Big|_{\bar{x}} = -\frac{||p+p_w-\breve{p}_i||}{2\beta^{\frac{3}{2}}}\Big|_{\bar{x}}$$

Now, that both process and measurement model are derived, can the EKF be stated. The equations are as following [22]:

$$\begin{aligned}
K_k &= \bar{P}_k C_k^T (C_k \bar{P} C_k^T + R_k)^{-1} \\
\hat{x}_k &= \bar{x}_k + K_k(y_k - h(\bar{x}_k))) \\
P_k &= (I_{n\times n} - K_k C_k)\bar{P}_k \\
\bar{x}_k &= A\hat{x}_{k-1} \\
\bar{P}_k &= AP_{k-1}A^T + D^T QD
\end{aligned}$$

where $Q \in \mathbf{R}^{n\times n}$ and $R \in \mathbf{R}^{m\times m}$ are the process and sensor noise covariance matrices, respectively. Further, corresponds n and m to the number of states and measurements. P_k is the covariance matrix. Note that $(\bar{\cdot})$ mark posterior estimates. Also, it should be noted that the first iteration, $k = 0$, are the initial values $\bar{x}_0$ and $\bar{P}_0$ used.

4.1 Observability Analysis

Observability means that we can recreate uniquely all states from the measurement vector y. If this is the case, then the observability matrix of the pair (A,C) have full rank, which means $rank(\mathscr{O}) = n$, where n is the number of states. The matrix is defined as following [10]:

$$\mathscr{O} = \begin{bmatrix} C_k \\ C_k A \\ \vdots \\ C_k A^{n-1} \end{bmatrix} \tag{8}$$

Assumption 3. *$m \geq 4$ pseudo-range measurement and all transponder positions is not co-planar.*

Lemma 1. *The pair (A,C) is observable for both Case A and B.*

Proof: It is trivial to calculate the observability matrix in Equation (8). For case A and B, investigating the rank shows that $rank(\mathscr{O}) = 4$ and $\mathscr{O} = 10$, respectively. That is if Assumption 3 is satisfied. From the full rank of Equation (8) in both Case A and B, can observability be concluded. q.e.d.

5 Case Study

This section will present a simulation study of Case A and B. The study includes the two EKF developed in Section 4 and they are implemented in Matlab. The two filters are compared and discussed. The number of transponders are $m = 4$ and are placed such that they are not co-planar with the following positioning:

$$\begin{aligned}
\breve{p}_1 &= \begin{bmatrix}15 & 0 & 1\end{bmatrix}^T, & \breve{p}_2 &= \begin{bmatrix}0 & 15 & 20\end{bmatrix}^T \\
\breve{p}_3 &= \begin{bmatrix}-15 & 0 & 5\end{bmatrix}^T, & \breve{p}_4 &= \begin{bmatrix}0 & -15 & 16\end{bmatrix}^T
\end{aligned}$$

The position of the receiver at the ROV is kept constant at $p = \begin{bmatrix}1 & 2 & 3\end{bmatrix}^T$. The measurements for Case A are generated from Equation (1) and correspondingly (3) for B. To simulate the wave motion p_w in Equation (3), a second order wave model was used. Parameters in the wave model are set to $\omega_0 = 0.8$, $\lambda = 0.1017$ and $\sigma_{wi} = 0.8367$ for $i = 1,2,3$. This means that the wave frequency estimated, is defined for a spectrum in each direction. The speed of sound bias in water is set to $\beta = 0.95$ for both cases. The measurement noise is $\sigma_m^2 = 1e-2$. The time step used for discretization and simulation is $\Delta t = 0.2$.

For the initialization of the EKF in Case A is $\bar{x}_0 = \begin{bmatrix}0_{1\times 3} & 1\end{bmatrix}^T$. Further, sensor noise matrix is $R = diag(\sigma_m^2, \sigma_m^2, \sigma_m^2, \sigma_m^2)$ and the process noise is $Q = diag(\sigma_p^2, \sigma_p^2, \sigma_p^2, \sigma_p^2, \sigma_\beta^2) \in \mathbf{R}^{4\times 4}$. Here are $\sigma_p^2 = 1e-4$ and $\sigma_\beta^2 = 1e-6$. The covariance matrix is initial set to $P_0 = diag(0.1, 0.1, 0.1, 1e-4) \in \mathbf{R}^{4\times 4}$.

For Case B the model is the initial states set to $\bar{x}_0 = \begin{bmatrix}0_{1\times 9} & 1\end{bmatrix}^T$. The sensor noise covariance matrix R is the same as in Case A, but the process noise covariance matrix is $Q = diag(1_{1\times 3}, \sigma_p^2, \sigma_p^2, \sigma_p^2, \sigma_p^2, \sigma_\beta^2) \in \mathbf{R}^{7\times 7}$. The inital covariance matrix is set to $P_0 = diag((1e-3)_{1\times 6}, (0.1)_{1\times 3}, 1e-4) \in \mathbf{R}^{10\times 10}$ where the subscripts denote dimensions.

RMS	$x[m]$	$y[m]$	$z[m]$	$beta[]$
EKF Case A	0.009	0.009	0.0336	0.0013
EKF Case B	0.013	0.013	0.049	0.0014

TABLE 1: **RMS ERROR FOR CASE A and B**

6 Simulation Results and Discussion

The simulation results from the case study in the previous section are presented in Table 1 and Figure 5-4. Both case A and B are run for 300 seconds.

Table 1 presents the Root Mean Square (RMS) for the position and bias estimation. It is apparent that the RMS performance

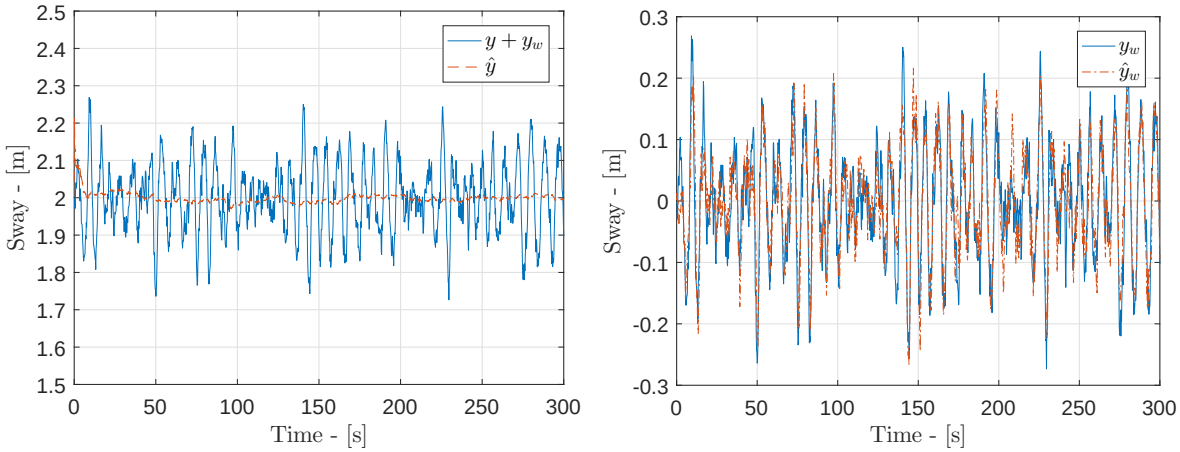

(a) **SWAY ESTIMATED POSITION.**

(b) **SWAY ESTIMATED WAVE POSITION.**

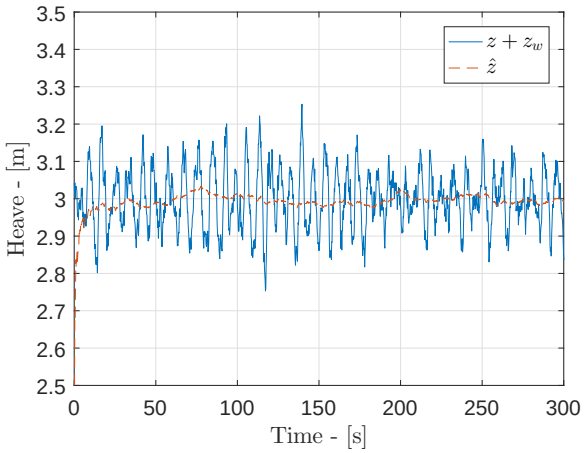

(c) **HEAVE ESTIMATED POSITION.**

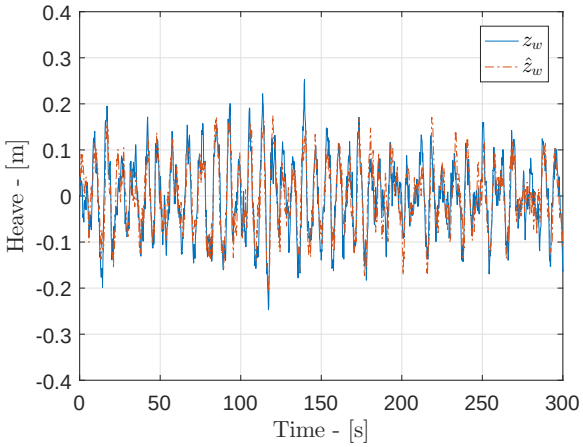

(d) **HEAVE ESTIMATED WAVE POSITION.**

FIGURE 4: **ESTIMATED STATES WITH EKF INCLUDING WAVE FILTER.**

is similar for the cases, with naturally slightly worse performance in Case B. Both A and B have a small RMS in surge, sway and heave. However, heave has a larger RMS, which is due to the short transponder placement in z-direction. The estimated biases have very similar RMS performance.

Figure 4 presents how the wave filtering implementation in Case B separates the wave and low-frequency motion in sway and heave as exemplified in Figure 2. Figure 4a has one plot showing the combination of real low and wave frequency motions, $y + y_w$, shown by a solid blue line. The other plot in the figure is estimated low-frequency motion, $\hat{y}$ in a red dashed line. From this, we can see that the estimate converges smoothly to the real position at $y = 2$, as defined in the simulation study. Further, the wave frequency motion is filtered away. It is important to note that the assumed noise variance is relatively low at $\sigma_p^2 = 1e-4$. Meaning that the model is trusted more than the measurements. This is good in this case since $\dot{p} = 0$. Figure 4b shows the simulated wave frequency y_w against estimated $\hat{y}_w$ in the blue solid line. Since the $\hat{y}_w$ is very similar to the simulated y_w means that we have a good estimate. The resulting estimates in heave motion are shown in Figure 4c and 4d. Here does also the heave position estimate, $\hat{z}$ converge towards $z = 3$. The convergence time seems to be a bit longer, but it can be explained by the transponder positions and that it is the state furthest away from the initial condition at $\bar{z} = 0$. The surge results are left out here since the result is very similar to the results in sway. Figure 5 shows how the covariance matrix converges towards steady state values. This effectively means that the filter converges. However, since the EKF is not proven globally stable, this can't be guaranteed. But this simulation shows how well the wave motion can be estimated.

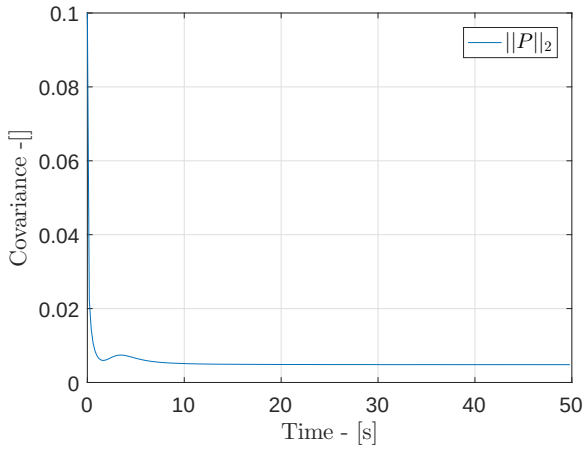

FIGURE 5: **NORM OF COVARIANCE MATRIX IN CASE B** ($||P||_2$)

7 Conclusion and Further Work

In this paper, a filter for underwater positioning in an aquaculture environment is presented. Demanding weather conditions will impose oscillations on the transponders near the surface area. An EKF solution has been proposed including a wave motion model integrated with pseudo-range measurements. This was simulated in Matlab with a predefined case study. The results show that the filter compensates for the wave motion and gives almost the same performance as a system without environmental disturbances. Further work will include experimental analyzes of real wave motion spectra. Fusion of more sensors integrated into the same filter will increase performance.

ACKNOWLEDGMENT

This work is funded by the Norwegian University of Science and Technology (NTNU), Norwegian Research Council projects Reducing Risk in Aquaculture (254913) and SFI Exposed (237790).

REFERENCES

[1] Bjelland, H. V., and et.al. "Exposed aquaculture in norway". In OCEANS 2015 - MTS/IEEE Washington, pp. 1–10.

[2] Christ, R. D., and Wernli Sr, R. L., 2013. *The ROV manual: a user guide for remotely operated vehicles*. Butterworth-Heinemann.

[3] Utne, I. B., Schjolberg, I., and Holmen, I. M., 2015. Reducing risk to aquaculture workers by autonomous systems and operations. i: Safety and reliability of complex engineered systems.

[4] Farrell, J., 2008. *Aided Navigation: GPS with High Rate Sensors*. McGraw-Hill Education.

[5] Kinsey, J. C., Eustice, R. M., and Whitcomb, L. L. "A survey of underwater vehicle navigation: Recent advances and new challenges". In IFAC Conference of Manoeuvering and Control of Marine Craft, Vol. 88.

[6] Leonard, J. J., and Bahr, A., 2016. *Autonomous Underwater Vehicle Navigation*. Springer International Publishing, Cham, pp. 341–358.

[7] Mahony, R., Hamel, T., and Pflimlin, J. M., 2008. "Nonlinear complementary filters on the special orthogonal group". *IEEE Transactions on Automatic Control,* ***53***(5), pp. 1203–1218.

[8] Grip, H. F., Fossen, T. I., Johansen, T. A., and Saberi, A., 2015. "Globally exponentially stable attitude and gyro bias estimation with application to gnss/ins integration". *Automatica,* ***51***, pp. 158–166.

[9] Markley, F. L., 2003. "Attitude error representations for kalman filtering". *Journal of Guidance, Control, and Dynamics,* ***26***(2), pp. 311–317.

[10] Chen, C.-T., 2013. *Linear system theory and design*, fourth edition. ed. The Oxford series in electrical and computer engineering. Oxford University Press, New York.

[11] Bancroft, S., 1985. "An algebraic solution of the gps equations". *IEEE Transactions on Aerospace and Electronic Systems,* ***AES-21***(1), pp. 56–59.

[12] Batista, P. "Ges long baseline navigation with unknown sound velocity and discrete-time range measurements". In 52nd IEEE Conference on Decision and Control, pp. 6176–6181.

[13] Johansen, T. A., and Fossen, T. I., 2016. "The exogenous kalman filter (xkf)". *International Journal of Control*, pp. 1–7.

[14] Johansen, T. A., Fossen, T. I., and Goodwin, G. C., 2016. "Three-stage filter for position estimation using pseudorange measurements". *IEEE Transactions on Aerospace and Electronic Systems,* ***52***(4), pp. 1631–1643.

[15] Johansen, T. A., and Fossen, T. I., 2016. "Nonlinear observer for tightly coupled integration of pseudorange and inertial measurements". *IEEE Transactions on Control Systems Technology,* ***24***(6), pp. 2199–2206.

[16] Stovner, B. B., Johansen, T. A., Fossen, T. I., and Schjolberg, I. "Three-stage filter for position and velocity estimation from long baseline measurements with unknown wave speed". In 2016 American Control Conference (ACC), pp. 4532–4538.

[17] Jorgensen, E. K., Johansen, T. A., and Schjolberg, I., 2016. "Enhanced hydroacoustic range robustness of three-stage position filter based on long baseline measurements with unknown wave speed*". *IFAC-PapersOnLine,* ***49***(23), pp. 61–67.

[18] Faltinsen, O. M., 1990. *Sea loads on ships and offshore structures*. Cambridge ocean technology series. Cambridge University Press, Cambridge.

[19] Balchen, J. G., Jenssen, N. A., and Saelid, S. "Dynamic positioning using kalman filtering and optimal control theory". In IFAC/IFIP symposium on automation in offshore oil field operation, Vol. 183, p. 186.

[20] Fossen, T. I., 2011. *Handbook of Marine Craft Hydrodynamics and Motion Control*. Wiley.

[21] Groves, P. D., 2008. *Principles of GNSS, inertial, and multi-sensor integrated navigation systems*. Artech House, Boston/ London.

[22] Brown, R. G., and Hwang, P. Y. C., 2012. *Introduction to Random Signals and Applied Kalman Filtering with Matlab Exercises, 4th Edition*. Introduction to random signals and applied Kalman filtering. John Wiley and Sons.